RESEARCH ARTICLE

J Anim Sci Technol 2022;64(6):1199-1214
https://doi.org/10.5187/jast.2022.e60

JAST
Journal of Animal Science and Technology
pISSN 2672-0191 eISSN 2055-0391

Apolipoprotein H: a novel regulator of fat accumulation in duck myoblasts

Ziyi Pan, Guoqing Du, Guoyu Li, Dongsheng Wu, Xingyong Chen* and Zhaoyu Geng*

College of Animal Science and Technology, Anhui Agricultural University, Hefei 230036, China

Received: Apr 7, 2022
Revised: Jul 7, 2022
Accepted: Jul 9, 2022

***Corresponding author**
Xingyong Chen
College of Animal Science and Technology, Anhui Agricultural University, Hefei 230036, China.
Tel: +86-15605510863
E-mail: chenxingyong@ahau.edu.cn

Zhaoyu Geng
College of Animal Science and Technology, Anhui Agricultural University, Hefei 230036, China.
Tel: +86-13075573377
E-mail: gzy@ahau.edu.cn

ORCID
Ziyi Pan
https://orcid.org/0000-0002-6013-2748
Guoqing Du
https://orcid.org/0000-0002-8635-471X
Guoyu Li
https://orcid.org/0000-0003-3967-8129
Dongsheng Wu
https://orcid.org/0000-0003-3276-9212
Xingyong Chen
https://orcid.org/0000-0001-8849-8891
Zhaoyu Geng
https://orcid.org/0000-0001-8939-6379

Competing interests
No potential conflict of interest relevant to this article was reported.

Abstract

Apolipoprotein H (APOH) primarily engages in fat metabolism and inflammatory disease response. This study aimed to investigate the effects of APOH on fat synthesis in duck myoblasts (CS2s) by APOH overexpression and knockdown. CS2s overexpressing APOH showed enhanced triglyceride (TG) and cholesterol (CHOL) contents and elevated the mRNA and protein expression of AKT serine/threonine kinase 1 (AKT1), ELOVL fatty acid elongase 6 (ELOVL6), and acetyl-CoA carboxylase 1 (ACC1) while reducing the expression of protein kinase AMP-activated catalytic subunit alpha 1 (AMPK), peroxisome proliferator activated receptor gamma (PPARG), acyl-CoA synthetase long chain family member 1 (ACSL1), and lipoprotein lipase (LPL). The results showed that knockdown of APOH in CS2s reduced the content of TG and CHOL, reduced the expression of ACC1, ELOVL6, and AKT1, and increased the gene and protein expression of PPARG, LPL, ACSL1, and AMPK. Our results showed that APOH affected lipid deposition in myoblasts by inhibiting fatty acid beta-oxidation and promoting fatty acid biosynthesis by regulating the expression of the AKT/AMPK pathway. This study provides the necessary basic information for the role of APOH in fat accumulation in duck myoblasts for the first time and enables researchers to study the genes related to fat deposition in meat ducks in a new direction.

Keywords: Apolipoprotein H, Myoblasts, Lipid metabolism, AKT/AMPK signalling pathway

INTRODUCTION

Duck is the second most frequently consumed type of poultry in Asia. The improvement of carcass characteristics and meat quality is beneficial to consumers. High intramuscular fat (IMF) in duck pectoral muscle is gradually gaining popularity among consumers and researchers in the poultry industry [1]. IMF mainly accumulates in muscle cells [2] and affects meat duck flavour, tenderness, and quality [3,4]. Lipids include triglycerides (TGs), phospholipids, and cholesterol (CHOL), which are insoluble in water, and their transport in the extracellular fluid, lymph, and blood requires proteins associated with the lipids to suspend them in water [5]. Therefore, IMF is a key indicator for evaluating duck meat quality and it is affected by proteins that interact with lipids.

Apolipoprotein H (APOH) binds to negatively charged phospholipids located in the cell core and attaches to the partial structure of various lipoproteins [6]. APOH is involved in several human

Funding sources
This work was financially supported by the Major Scientific and Technological Special Project in Anhui Province (201903a06020018).

Acknowledgements
The authors would like to acknowledge the owners of Anhui Qiangying Duck Industry Co., Ltd., in Anhui Province, China, for proving duck embryos.

Availability of data and material
Upon reasonable request, the datasets of this study can be available from the corresponding author.

Authors' contributions
Conceptualization: Chen X, Geng Z.
Data curation: Du G, Li G.
Formal analysis: Wu D.
Methodology: Pan Z.
Software: Pan Z.
Validation: Pan Z.
Investigation: Geng Z.
Writing - original draft: Pan Z, Chen X.
Writing - review & editing: Pan Z, Du G, Li G, Wu D, Chen X, Geng Z.

Ethics approval and consent to participate
The animal experiment was reviewed and approved by the Institutional Animal Care and Use Committee of Anhui Agriculture University (no. SYDW-P20190600601). The experiments were performed in accordance with the Regulations for the Administration of Affairs Concerning Experimental Animals and the Standards for the Administration of Experimental Practices.

physiological processes, such as lipid metabolism, proliferation, inflammation, thrombosis, systemic lupus erythematosus, cognitive aging, metabolism of TG in protein lipoprotein lipase (LPL), and participation in the immune response process of anti-phospholipid syndrome (APS) [7–14]. LPL has important functions in lipid metabolism, such as participation in fatty acid transport and TG hydrolysis [15,16]. APOH has been reported to inhibit peroxisome proliferator activated receptor gamma (PPARG) expression and increase LPL activity in macrophages[17–19]. PPARG has positive effects not only in regulating cellular lipid metabolism but also in cytokine production and inflammation inhibition [20]. Apolipoprotein plays an essential role in the two stages of chicken skeletal muscle myogenesis and adipogenesis [2], and the PPAR pathway is involved in lipid deposition in chicken skeletal muscle [21]. However, few studies have addressed the mechanisms involved in regulating lipid metabolism in duck myoblasts.

A previous study showed that APOH is the difference gene between high and low groups of meat ducks with residual feed intake, and the factor affecting the residual feed intake of meat ducks is lipid metabolism [22]. Therefore, the APOH gene may play an important role in duck lipid metabolism. To clarify the key role of APOH gene in the lipid metabolism of duck myoblasts, this study constructed a cell model of APOH gene knockdown and overexpression and detected the intracellular conditional factors and indicators for analysis. This study provides a molecular basis for breeding ducks with high IMF by explaining the molecular mechanism of APOH gene promoting fat accumulation in duck myoblasts.

MATERIALS AND METHODS

Animals

The animal experiment was reviewed and approved by the Institutional Animal Care and Use Committee of Anhui Agriculture University (no. SYDW-P20190600601). Duck myoblasts were isolated from thoracic tissue of 13 embryonic-day-old duck embryos. Duck embryos are provided by Qiangying Duck Industry, Anhui.

Primary cell isolation, identification and culture

The breast tissues of 12 duck embryos that had been hatched for 13 days were removed, cut into pieces, added with five times the volume of type I collagenase and digested in a 37℃ water bath for 2 h. After digestion until there is no large tissue clumps, a equal volume of Dulbecco's Modified Eagle Medium (DMEM)/F12 (Biological Industries, Kibbutz Beit-Haemek, Israel) was added to terminate digestion. Collect the digested tissue supernatant, filter it through a 300-mesh filter, and collect the filtrate. The filtrate was collected into a 15 mL centrifuge tube, centrifuged at 1,000 rpm/min for 10 min, collect the cell precipitation, 2 mL of culture medium was added to resuspend the cells, and the cells were collected by centrifugation again under the same conditions. Ten millilitres of complete medium (79% DMEM/F12 medium + 20% fetal bovine serum [FBS; Biological Industries] + 1% antibiotics [Thermo Fisher Scientific, Waltham, MA, USA]) was added to the cells (CS) to resuspend and seed them in a 10 cm petri dish and then they were incubated at 37℃ for 4 h.

A large number of myoblasts (CS1) and a small number of other cells were in a nonadherent state. To obtain purer myoblasts, the culture of the supernatant from the first culture dish was repeated and cultured for 4 h. Finally, the supernatant from the second dish was collected, the number of cells (CS2s) was recorded and they were seeded in 6-well plates. Medium containing 89% DMEM/F12, 10% FBS and 1% antibiotics was used to culture the CS. The incubator conditions were 37℃ and 5% CO_2.

https://doi.org/10.5187/jast.2022.e60

When cells grew to 80% confluence, they were reseeded into 24-well plates for immunofluorescence staining of PAX7 (Proteintech, Wuhan, China) [22,23]. The cells were fixed for 15 min with 4% paraformaldehyde (Biosharp, Hefei, China), blocked, and incubated with anti-paired box (PAX7) primary antibody at 4℃ overnight. The anti- PAX7 was detected with a secondary antibody labeled with fluorescein isothiocyanate (FITC) (Immunoway, Plano, TX, USA) in a darkroom at 25℃ for 1 h. Finally, the cells were incubated with 4′,6-diamidino-2-phenylindole (DAPI) (Servicebio, Wuhan, China) in the darkroom for 15 min. Then the immunofluorescence images of PAX7 protein labeled were observed by fluorescence microscope (DP73, Olympus, Tokyo, Japan).

Plasmid construction and cell transfection

The duck APOH (XM_005016097.5) coding region was amplified with forward primer 5`-GGATCCATGTACTCCCTGGTGCTGGTCG -3` (contain BamHI restriction site) and reverse primer 5`-GCTAGCTCATTCATGATCTTCACATGGTTTC-3` (contain NheI restriction site). Polymerase chain reaction (PCR) (T100, Bio-Rad, Hercules, CA, USA) was used to amplify a 1065 bp product and it was purified. The APOH sequence and pBI-CMV3 vector containing BamHI (NEB, Beijing, China) and NheI (NEB) restriction endonuclease cleavage sites were digested and ligated together (a gift from Zhao Zhihui's research group at Guangdong Ocean University). The plasmid pBI-CMV3-APOH was double-enzyme digested and confirmed by agarose gel electrophoresis. Shanghai Sangon Biotechnology Co., Ltd. sequenced the plasmid to validate it.

APOH interfering RNA (shRNA) was designed according to its mRNA sequence (XM_005016097.5) with online software (https://www.thermofiser.com/us/en/home/brands/invitrogen/ambion.html), and APOH-shRNA interference sequences (5`-AGAGGTCTTCG CCACAATCAATGTTCAAGAGACATTGATTGTGGCGAAGAGCTTTTTTG-3` and 5`- GATCCAAAAAAGCTCTTCGCCACAATCAATGTCTCTTGAACATT GATTGTGGCGAAGAGC-3`) were synthesized. The shRNA annealed product was purified and ligated into pGPU6-GFP-Neo knockdown vector (a gift from Zhao Zhihui Research Group at Guangdong Ocean University).

When the cells grew to 70%–80% confluence, we transfected them with the overexpression, knockdown, and normal control plasmids of APOH with Exfect, with at least three replicates per treatment. After 24 h of transfection, the corresponding experiment was carried out.

Real-time polymerase chain reaction

Then, total RNA was extracted by TRIzol (Thermo Fisher Scientific). cDNA (1 μg) was reverse transcribed using an RT-cDNA synthesis kit (Vazyme, Nanjing, China). PCR mix (Vazyme) was used in the real-time PCR assay. The reaction system was 95℃ for 5 min, 95℃ for 30 s, and 60℃ for 30 s for 35 cycles. With glyceraldehyde 3-phosphate dehydrogenase (GAPDH) as the reference gene, quantitative PCR was used to detect the gene's mRNA level. Shanghai Shenggong Biotechnology Co., Ltd. synthesized the RT-PCR primers (Table 1). GAPDH was used as the reference gene, and an experiment was performed in triplicate. The relative expression of genes was calculated using $2^{-\Delta\Delta Ct}$.

Detection of protein expression by western blotting

Cells were harvested 24 hours after transfection of the plasmid. After aspirating the medium, the cells were scraped off with a cell scraper and collected into a centrifuge tube after washing with phosphate-buffered saline (PBS). The centrifuge tube containing cells was centrifuged, the supernatant was removed, RIPA protein lysis buffer and protease inhibitors were added, and the

Table 1. List of primer sequences used for qRT-PCR

Genes		Primer sequences (5'-3')	Product (bp)	Temperature (℃)
APOH	F	AAAAGTCTGTTCCAAGCCACC	249	58.5
	R	GGCACAGGAGCGTGTTGAG		
AKT1	F	AGGTTAGGTGGCGGTCCTGATG	225	60
	R	GCGGTTCCACTGGCTGAATAGG		
AMPK	F	CGACAGAAGATTCGCAGCCTTG	232	52
	R	TGTGACAGTAATCCACGCCAGA		
ACC1	F	GGTCCTCCAAGCCAAGCAATGT	201	57
	R	CGAAGACCACTGCCACTCCAAG		
PPARG	F	GCCACAAGCGGAGAAGGAGAAG	186	53
	R	GCAGCGGTGACACATGCTTACA		
ACSL1	F	CGTTACTCCACCGAGGCTTCAA	115	56
	R	TCATAGAGCGGCACCACTACCA		
ELOVL6	F	CAGTCAGTGTGCGACCAGAGTT	226	60
	R	CCAGCCACCATGTCCTTGTAGG		
FAS	F	CCTACTAAGCAGCCTGAGAATG	130	55
	R	AGATTGTCCGCCTTCCTGAT		
LPL	F	CCAAGACCAACCAGCCATTCCT	243	60
	R	CGCCTGACTTCACTCTGACTCT		
GAPDH	F	GGAGAAACCAGCCAAGTAT	177	60
	R	CCATTGAAGTCACAGGAGA		

qRT-PCR, quantitative real-time polymerase chain reaction; bp, base pair; APOH, apolipoprotein H; AKT1, AKT serine/threonine kinase 1; AMPK, AMP-activated catalytic subunit alpha 1; ACC1, acetyl-CoA carboxylase 1; PPARG, peroxisome proliferator activated receptor gamma; ACSL1, acyl-CoA synthetase long chain family member 1; ELOVL6, ELOVL fatty acid elongase 6; FAS, fas cell surface death receptor; LPL, lipoprotein lipase; GAPDH, glyceraldehyde 3-phosphate dehydrogenase.

cells were lysed for 10 min on ice. The lysed cells were centrifuged at 13,000 rpm/min (4℃) for 10 minutes to obtain a supernatant containing total protein. To keep the sample loading consistent, bicinchoninic acid (BCA) kits were used for protein concentration detection and quantification of total protein. For western blotting (PowerPac™ HV, Bio-Rad), consistent amounts of protein were separated by sodium dodecyl sulfate polyacrylamide gel electrophoresis (SDS-PAGE) and then the total protein was transferred to polyvinylidene difluoride (PVDF) (88518, Thermo Fisher Scientific) membranes. PVDF was incubated with 1% bovine serum albumin (BSA) for 2 h at room temperature and washed with tris-buffered saline (TBST). Then, the membrane was incubated with primary anti-APOH (1:1,000) antibody overnight at 4℃. Primary antibodies (ACC1, ACSL1, PPARG, LPL, ELOVL6, AKT, Pakt, AMPK, pAMPK) were diluted at a dilution ratio of 1:1,000. After the primary antibody was incubated and washed three times with TBST, the anti-rabbit secondary antibody (Immunoway) was incubated for 2 h. Enhanced chemiluminescence horseradish peroxidase (HRP) substrate was used to observe the stained protein bands. After taking an image with a chemiluminescence instrument, ImageJ was used to scan the gray value of the proteins.

Oil red O staining

Oil red O stock solution and working solution was prepared according to the previous research method [23].

After 24 h of transfection, the cells were washed with PBS after aspirating the cell culture

https://doi.org/10.5187/jast.2022.e60

medium. Cells were incubated with 4% paraformaldehyde (Biosharp, Hefei, China) for 30 min and washed three times with PBS. The washed cells were stained with Oil red O working solution at room temperature for 30 min, the Oil red O working solution was removed, 60% isopropanol was used to wash the cells three times, and finally the cells were washed three times with PBS. Then, 200 μL of 60% isopropanol was added to the cells for 20 min, and a microplate reader was used to measure the absorbance at 510 nm.

Analysis of intracellular triglyceride and cholesterol content

According to the kit instructions, the TG (Applygen, Beijing, China) and CHOL (Applygen, China) contents in CS2s were detected. The CS2 cells were collected 24 h after transfection with the plasmids. Cell numbers of different samples were unified by BCA protein quantification and three experiments were repeated for each model. TG and CHOL in the cell were normalized to the protein content. Use a microplate reader to measure the absorbance of different samples at a specific absorbance, and calculate the content of TG and CHOL.

Statistical analysis

Error bars in experimental results show mean ± standard error Statistically significant differences were defined as $p < 0.05$. Two-tailed (unpaired) t-tests method in GraphPad Prism 9 software (GraphPad software, San Diego, CA, USA) were used for data analysis in this study.

RESULTS

Cell isolation, identification and culture

After 24 h, the cells began to adhere to the wall and became spindle cells. Most of the CS2s extended at both ends after culturing for 36 h. After 48 h, they entered the logarithmic growth phase (Figs. 1A–1C). The cells were identified with the CS2-specific marker PAX7 for immunofluorescence identification (Figs. 1D–1F).

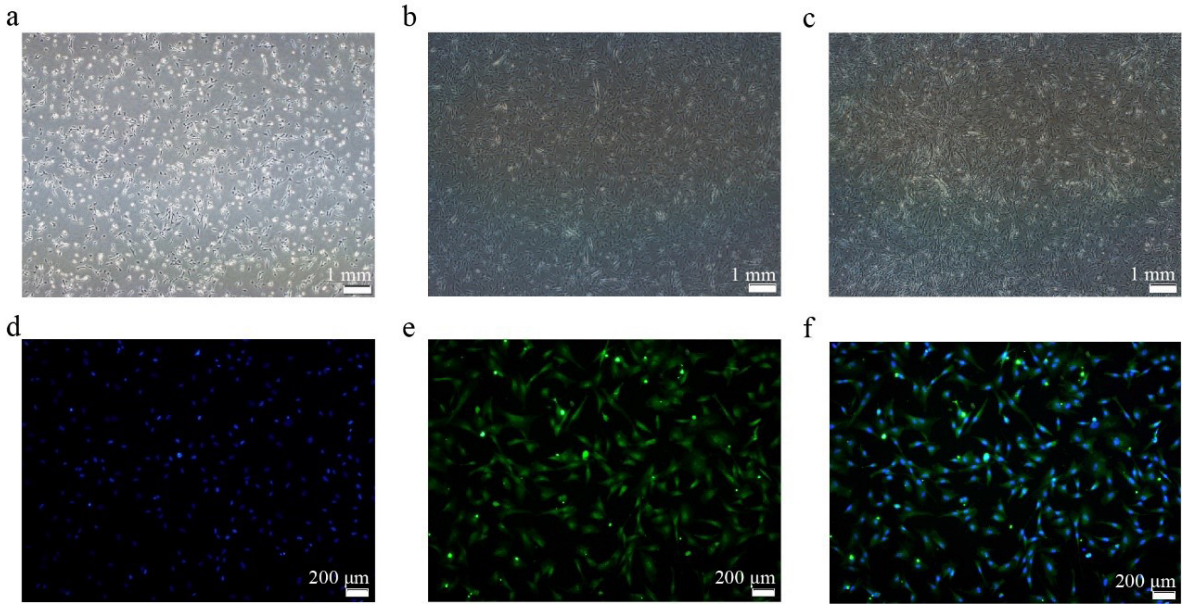

Fig. 1. CS2s separation and identification. (a) Cell morphology after 24 h of separation. (b) Cell morphology after 36 h of separation. (c) Cell morphology after 48 h of separation. (d) DAPI (blue). (e) PAX7 protein signal (green). (f) Merge image. CS2s, duck myoblasts; DAPI, 4′,6-diamidino-2-phenylindole; PAX7, paired box 7.

Construction of apolipoprotein H expression vector

The vector of overexpression (pBI-CMV3-APOH) and knockdown (pGPU6-GFP-Neo-APOH) APOH gene were constructed to examine the function of APOH in CS2s. The restriction enzyme digestion verification (Fig. 2C) shows that we successfully cloned the 1,053 bp duck APOH and constructed a recombinant expression vector. Sequencing technology confirmed that the

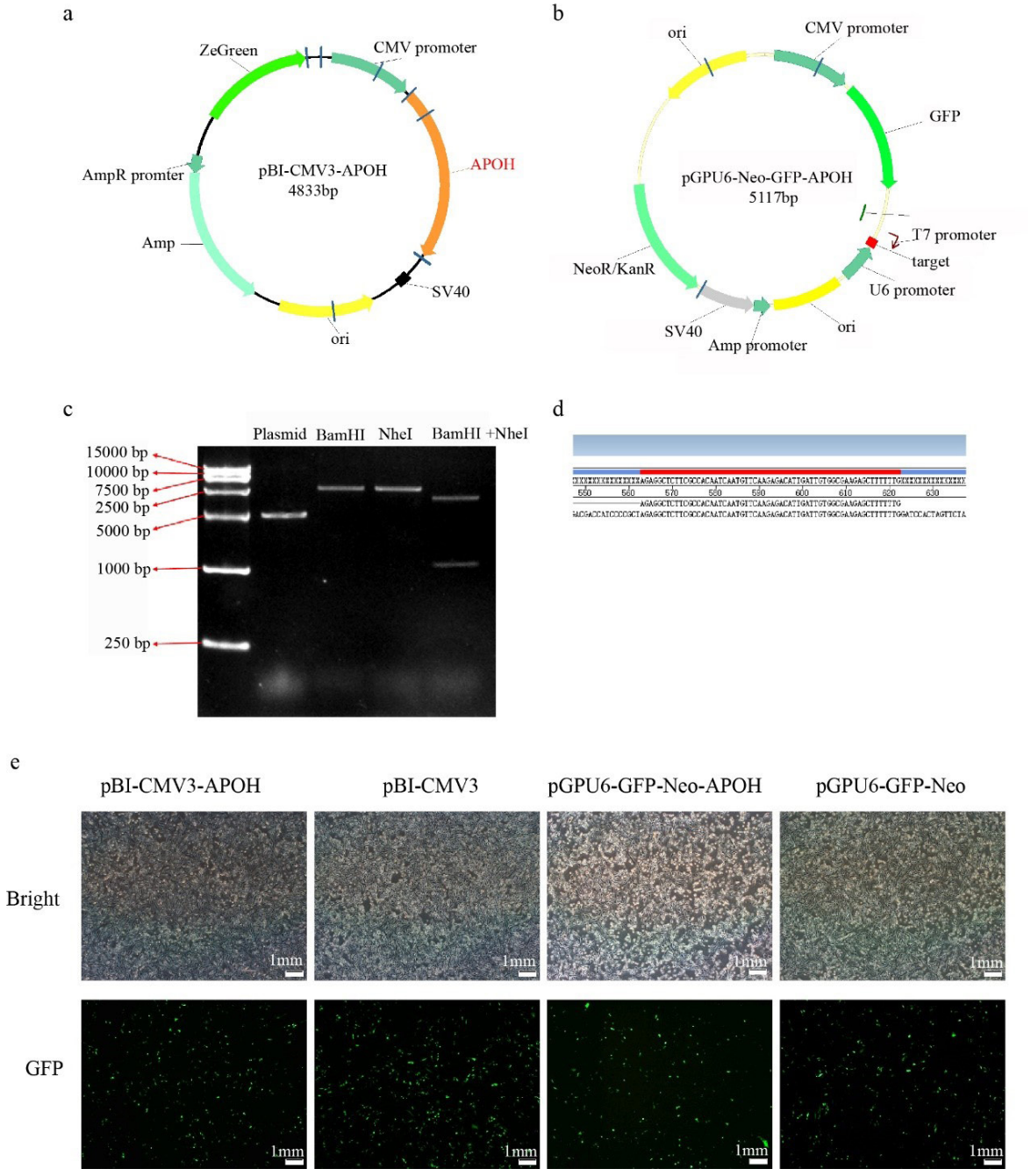

Fig. 2. Construction of the APOH gene overexpression vector and the interference vector. (a) Construction of the pBI-CMV3-APOH vector. (b) Construction of the pGPU6-GFP-Neo-APOH vector. (c) Enzymatic digestion verified the correct recombination of pBI-CMV3-APOH: The first lane is the size marker; Plasmid: pBI-CMV3 plasmid; BamHI: pBI-CMV3-APOH digested by BamHI; NheI, pBI-CMV3-APOH digested by BamHI; BamHI+NheI, pBI-CMV3-APOH digested by BamHI and NheI. (d) Sequence alignment of the interference target sequence and pGPU6-GFP-Neo-APOH. (e) Microscopic observation of CS2s transfected with the pBI-CMV3-APOH, pBI-CMV3, pGPU6-GFP-Neo-APOH, and pGPU6-GFP-Neo vectors. bp, base pair; APOH, apolipoprotein H.

https://doi.org/10.5187/jast.2022.e60

interference target sequence was successfully recombined into pGPU6-GFP-Neo (Fig. 2D).

After successful construction, the pBI-CMV3-APOH, pBI-CMV3, pGPU6-GFP-Neo-APOH, and pGPU6-GFP-Neo vectors were transfected into the CS2s when they attained 80% confluency. After 24 h of transfection, green fluorescent proteins were observed in the cells under an inverted fluorescence microscope (Fig. 2E). The results showed that the APOH gene overexpression and knockout myoblast model was successfully constructed.

The expression of apolipoprotein H mRNA and protein in transfected CS2s

After transfection with pBI-CMV3-APOH, pGPU6-GFP-Neo-APOH, and the corresponding empty vector for 24 h, the cells were collected, and the total RNA was extracted. RT-PCR and western blot were used to detect the mRNA and protein expressions of APOH in CS2s. The results showed that the mRNA expression of APOH gene in cells transfected with pBI-CMV3-APOH was significantly increased; the mRNA expression of APOH gene transfected with pGPU6-GFP-Neo-APOH was significantly lower than that transfected with empty vector (Figs. 3A and 3D).

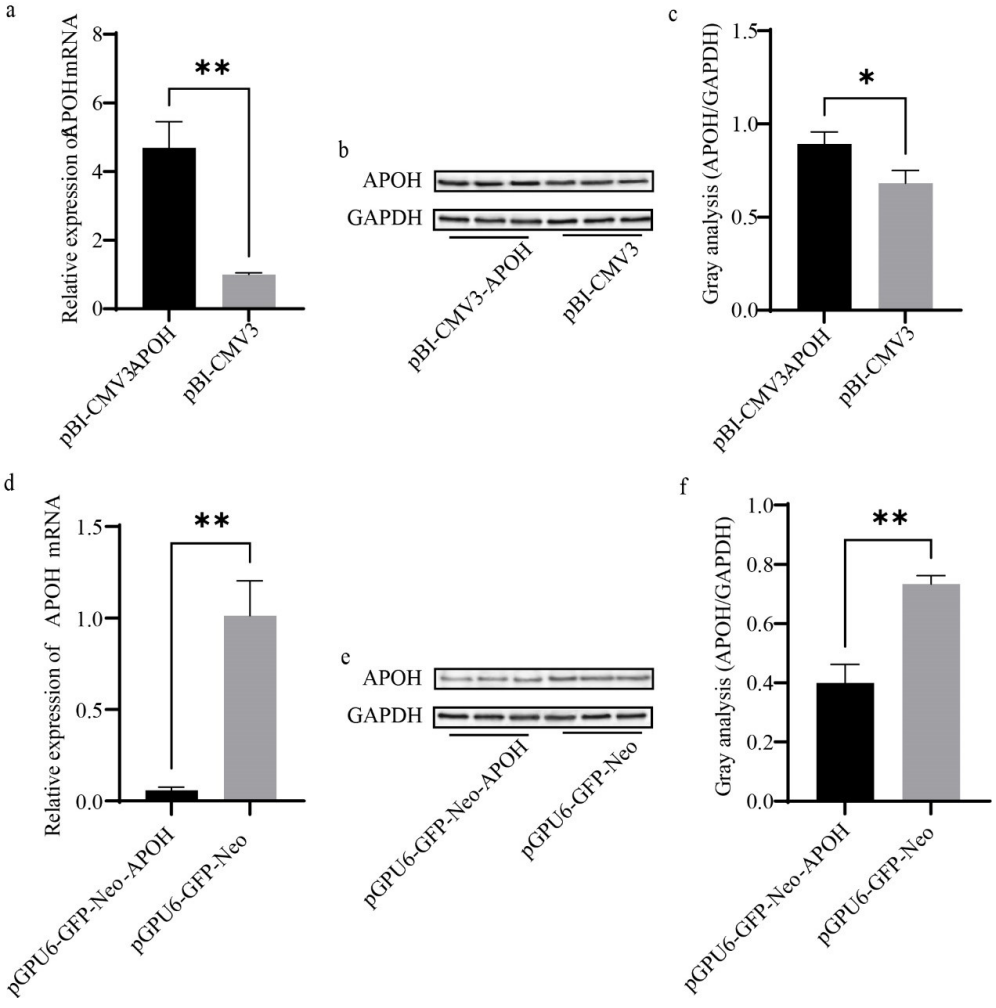

Fig. 3. The mRNA and protein expression levels of APOH in CS2s (n=3) after transfection with pBI-CMV3-APOH and pGPU6-GFP-Neo-APOH. (a), (d) Relative mRNA expression levels of APOH in CS2s transfected with pBI-CMV3-APOH and pGPU6-GFP-Neo-APOH vectors. (b), (e) The indicated protein levels were detected by western blotting analysis. (c), (f) Relative folds of APOH (protein/GAPDH) from the western blots in (b), (e) were quantified by a greyscale scan. Data are the mean ± SD from three independent experiments. *$p < 0.05$, **$p < 0.01$. CS2s, duck myoblasts; APOH, apolipoprotein H; GAPD, glyceraldehyde 3-phosphate dehydrogenase.

In CS2s transfected with pBI-CMV3-APOH, APOH protein overexpression was confirmed by western blot analysis (Figs. 3B and 3C). However, after pGPU6-GFP-Neo-APOH transfection, APOH protein expression was significantly reduced in CS2. (Figs. 3E and 3F).

Oil red O staining

Oil red O staining was observed under an optical microscope showed that a large number of red lipid droplets appeared in CS2s of the pBI-CMV3-APOH group, and the lipid droplet area was larger than that of the pBI-CMV3 group, while a small number of red lipid droplets appeared in the CS2s of the pGPU6-GFP-Neo-APOH group, and most of them were in a diffuse state (Fig. 4A). Further lipid content determination results showed that the lipid content of the pBI-CMV3-APOH group was significantly higher than that of pBI-CMV3 group, while the lipid content was significantly reduced after knockdown of the of the APOH gene in cells (Fig. 4B).

The contents of triglyceride and cholesterol in CS2s

We examined the effect of APOH on the synthesis of TG in CS2s by detecting the content of TG in CS2s. Levels of TG were higher in CS2s transfected with pBI-CMV3-APOH than in those transfected with the pBI-CMV3 vector (Fig. 5A). The TG content was lower in CS2s transfected with pGPU6-GFP-Neo-APOH than in the control group, which was transfected with only the pGPU6-GFP-Neo vector (Fig. 5C). Levels of CHOL were detected with a CHOL kit. The results showed that CHOL content was higher in CS2s transfected with pBI-CMV3-APOH than in the pBI-CMV3 group (Fig. 5B) and CHOL content was lower in CS2s transfected with pGPU6-GFP-Neo-APOH than in the pGPU6-GFP-Neo group (Fig. 5D).

Apolipoprotein H mRNA expression influences lipid metabolism-related genes in CS2s

After transfection with plasmids for 24 h, the mRNA and protein of lipid metabolism-related genes in CS2 cells were detected. The results showed that compared with the control group, AKT1,

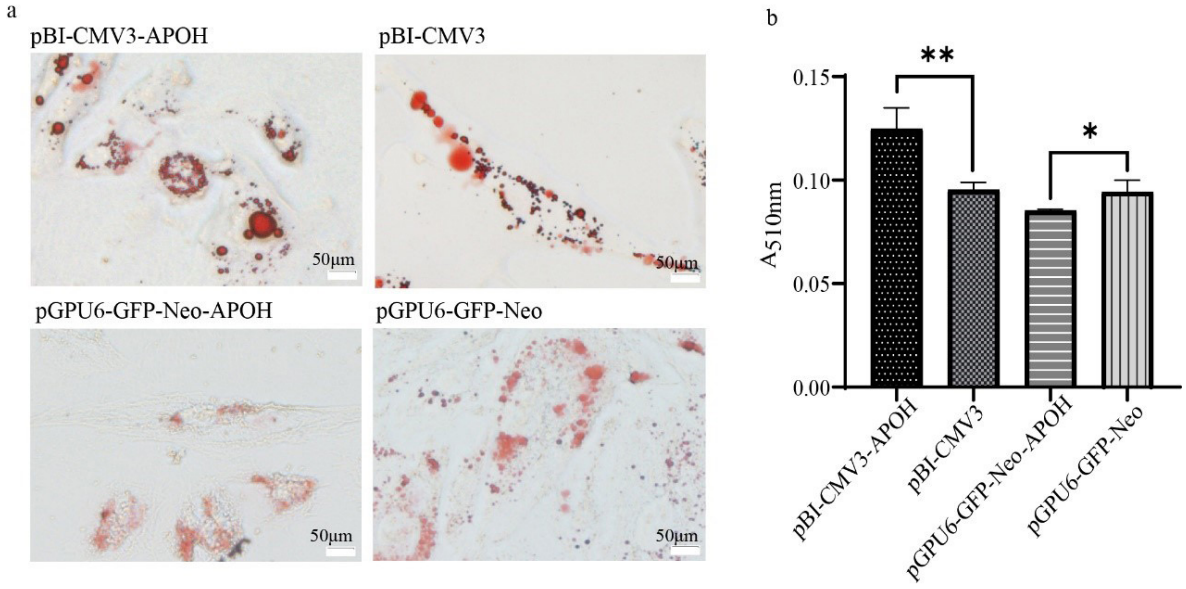

Fig. 4. Oil red O staining to observe the effect of APOH on cell lipid content in CS2s (n=3). (a) Lipid droplets in CS2s. (b) Quantitative results of lipid droplets in CS2s. Experimental data are shown as the mean ± SD. *$p < 0.05$, **$p < 0.01$. CS2s, duck myoblasts; APOH, apolipoprotein H.

https://doi.org/10.5187/jast.2022.e60

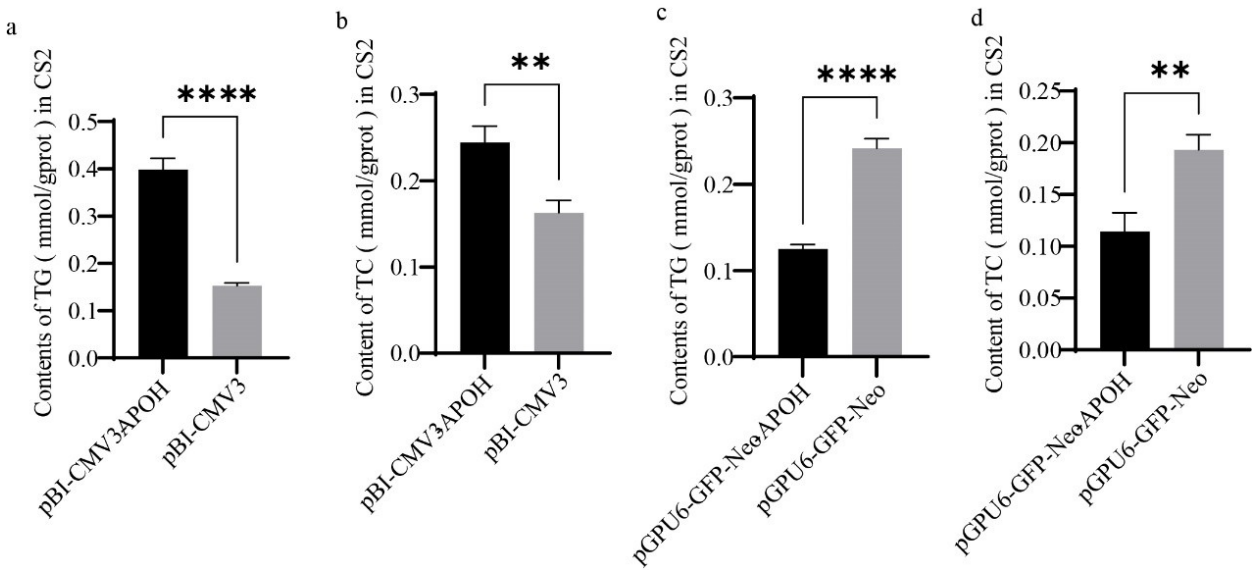

Fig. 5. Effect of APOH on TG and CHOL contents in CS2s. (a), (c) TG content in CS2s (n=3) transfected with the pBI-CMV3-APOH, pBI-CMV3, pGPU6-GFP-Neo-APOH, or pGPU6-GFP-Neo vectors. (b), (d) CHOL content in CS2s transfected with the pBI-CMV3-APOH, pBI-CMV3, pGPU6-GFP-Neo-APOH, or pGPU6-GFP-Neo vectors. Experimental data are shown as the mean ± SD. $^{**}p < 0.01$, $^{****}p < 0.0001$. CS2s, duck myoblasts; APOH, apolipoprotein H; TG, triglyceride; CHOL, cholesterol.

ACC1 and ELOVL6 genes were significantly up-regulated after overexpression of APOH gene in myoblasts, fas cell surface death receptor (FAS) gene had no significant change, while AMPK, PPARG, ACSL1 and LPL genes were significantly down-regulated. (Fig. 6A). A contrary result was obtained when CS2s were transfected with pGPU6-GFP-Neo-APOH. When CS2s were transfected with pGPU6-GFP-Neo-APOH, the genes involved in lipid metabolism including AKT1, ACC1 and ELOVL6 were significantly down-regulated, the expression of FAS had no significant change, and the gene expression of AMPK, PPARG, ACSL1 and LPL was significantly increased (Fig. 6B). The above results indicate that APOH gene plays an important role in the lipid metabolism mechanism of ducks.

The effect of apolipoprotein H on the relative protein expression of lipid metabolism-related genes in CS2s

Western blotting was used to evaluate the effect of APOH gene on the protein expression levels of lipid metabolism genes in CS2s. Overexpression of APOH increased the protein expression of ACC1 and ELOVL6 and decreased AMPK, PPARG, ACSL1, and LPL, but there was no significant difference in the total protein content of AKT (Figs. 7A and 7B). Overexpression of APOH increased the phosphorylation of AKT protein and simultaneously decreased the phosphorylation of AMPK protein (Figs. 7A, 7C, and 7D).

Knockdown of APOH decreased the protein expression of ACC1 and ELOVL6 and increased AMPK, PPARG, ACSL1, and LPL, but there was no significant difference in the total protein content of AKT (Figs. 8A and 8B). Knockdown of APOH decreased the phosphorylation of AKT protein and simultaneously increased the phosphorylation of AMPK protein (Figs. 8A, 8C, and 8D).

DISCUSSION

Meat duck skeletal muscle tissue is an important place for the utilization and oxidation of glucose

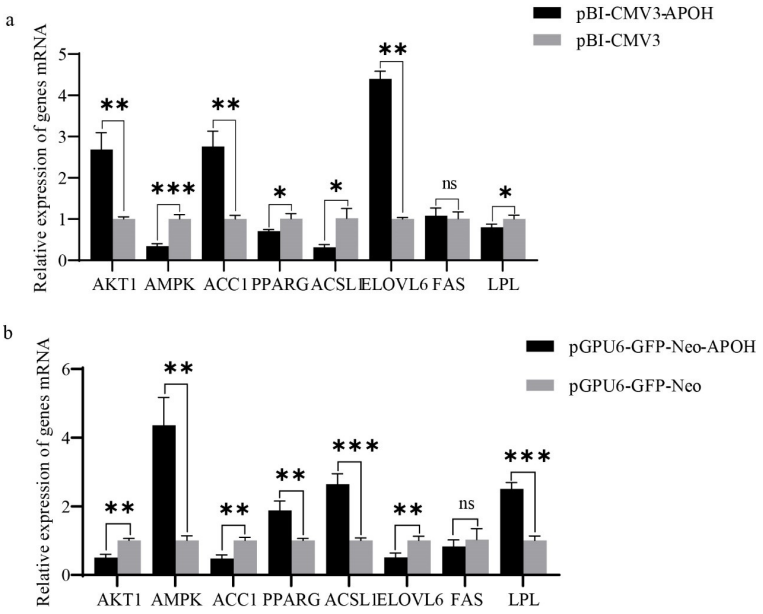

Fig. 6. Relative mRNA expression of lipid metabolism-related genes in CS2s (n=3). (a) Relative mRNA expression of lipid metabolism genes in CS2s after transfection with pBI-CMV3-APOH and pBI-CMV3. (b) Relative mRNA expression of lipid metabolism genes in CS2s after transfection with pGPU6-GFP-Neo-APOH and pGPU6-GFP-Neo. Data are the mean ± SD from three experiments, ns $p > 0.05$, *$p < 0.05$, **$p < 0.01$, ***$p < 0.001$. CS2s, duck myoblasts; AKT1, AKT serine/threonine kinase 1; AMPK, AMP-activated catalytic subunit alpha 1; ACC1, acetyl-CoA carboxylase 1; PPARG, peroxisome proliferator activated receptor gamma; ACSL1, acyl-CoA synthetase long chain family member 1; ELOVL6, ELOVL fatty acid elongase 6; FAS, fas cell surface death receptor; LPL, lipoprotein lipase.

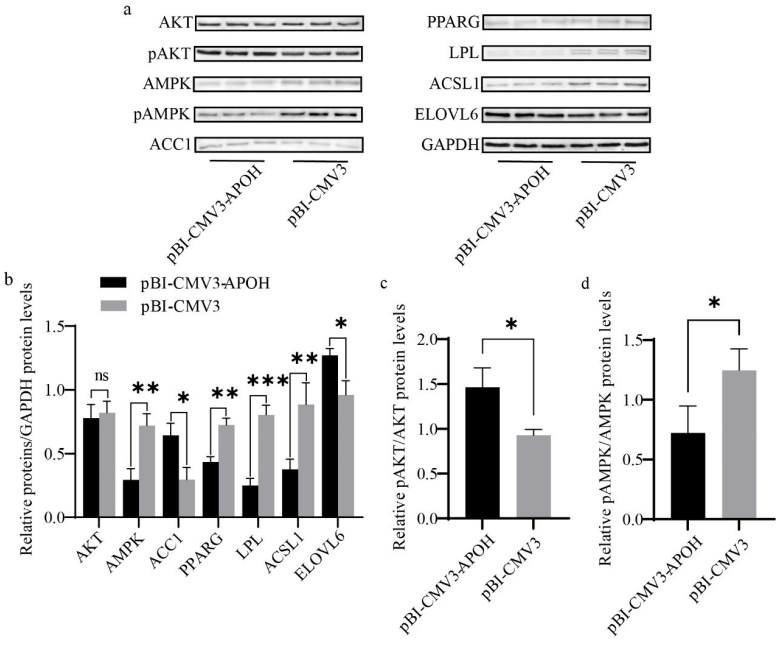

Fig. 7. The effect of overexpression of APOH gene on the expression of lipid metabolism-related proteins in CS2s (n=3). (a) Western blot showing the protein expression of lipid metabolism-related genes after transfection with pBI-CMV3-APOH and pBI-CMV3. (b) Relative folds of protein levels (proteins/GAPDH) from the western blots in (a) were quantified by a greyscale scan. (c) pAKT/AKT ratios from the western blots in (a) were quantified by a greyscale scan. (d) pAMPK/AMPK ratios from the western blots in (a) were quantified by a greyscale scan. Data are the mean ± SD from three experiments. ns $p > 0.05$, *$p < 0.05$, **$p < 0.01$, ***$p < 0.001$. CS2s, duck myoblasts; AKT1, AKT serine/threonine kinase 1; AMPK, AMP-activated catalytic subunit alpha 1; ACC1, acetyl-CoA carboxylase 1; PPARG, peroxisome proliferator activated receptor gamma; LPL, lipoprotein lipase; ACSL1, acyl-CoA synthetase long chain family member 1; ELOVL6, ELOVL fatty acid elongase 6.

https://doi.org/10.5187/jast.2022.e60

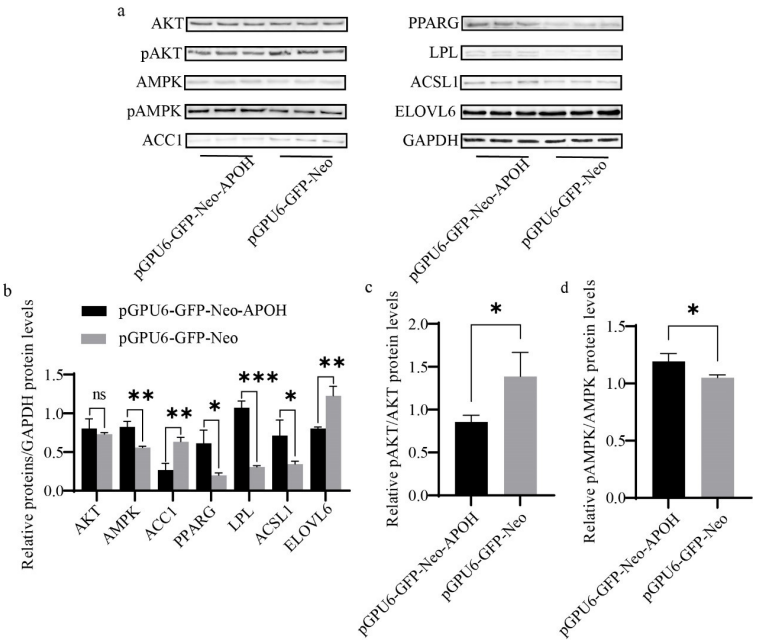

Fig. 8. Effect of knock-down APOH gene on the expression of lipid metabolism-related proteins in CS2s (n=3). (a) Western blot showing the protein expression of lipid metabolism-related genes after transfection with pGPU6-GFP-Neo-APOH and pGPU6-GFP-Neo. (b) Relative folds of protein levels (proteins/GAPDH) from the western blots in (a) were quantified by a greyscale scan. (c) pAKT/AKT ratios from the western blots in (a) were quantified by a greyscale scan. (d) pAMPK/AMPK ratios from the western blots in (a) were quantified by a greyscale scan. Data are the mean ± SD from three experiments, nss $p > 0.05$, *$p < 0.05$, **$p < 0.01$, ***$p < 0.001$. CS2s, duck myoblasts; AKT1, AKT serine/threonine kinase 1; AMPK, AMP-activated catalytic subunit alpha 1; ACC1, acetyl-CoA carboxylase 1; PPARG, peroxisome proliferator activated receptor gamma; LPL, lipoprotein lipase; ACSL1, acyl-CoA synthetase long chain family member 1; ELOVL6, ELOVL fatty acid elongase 6.

and fatty acids and an essential tissue for maintaining blood sugar balance. Although the lipid content in skeletal muscle cells is low, skeletal muscle cells can accumulate fat and are central to fat metabolism [24]. The changes in fat metabolism affect physiological processes such as cell growth and differentiation [25]. Among these, the synthesis of TGs is a vital process of the cell. Insulin resistance and type 2 diabetes in skeletal muscle are closely related to the accumulation of TGs in skeletal muscle [26,27]. A short-term high-fat overfeeding (HFO) diet has the most significant increase in methylation of human myoblasts, including the APOH gene, and DNA methylation can affect gene expression and chromosome stability, which may affect the phenotypic results of health and disease[28]. The lower abundance of APOH gene in chicken breast muscle indicates decreased of IMF content, and the mechanism is not clear[29, 30]. APOH is one of the key proteins in lipid metabolism. How does APOH regulate the synthesis and metabolism of lipids in myoblasts to avoid lipid accumulation and prevent lipotoxicity? The study of lipid metabolism in myoblasts is significant, so we used duck myoblasts as a lipid metabolism model for meat ducks.

Previous studies have shown a positive correlation between APOH and TG and CHOL [31]. This adds favourable evidence to our research results and indicates that APOH affects the TG and CHOL contents in myoblasts. Overexpression of APOH in myoblasts (CS2s) increased the contents of TG and CHOL. Furthermore, the inhibition of APOH expression in CS2s suppressed the TG and CHOL contents. The homeostasis of lipid metabolism throughout the nucleus depends on the regulation of these signals to form both complex and elaborate signal transduction pathways.

ACC1 is a multifunctional enzyme containing biotin that catalyses acetyl-CoA carboxylation to malonyl-CoA, the rate-limiting enzyme for malonyl-CoA fatty acid synthesis. ACC1 is regulated

by phosphorylation/dephosphorylation of serine residues [32]. The results of this study show that the expression of APOH plays a key role in regulating AKT/AMPK phosphorylation in myoblasts. AMPK is an upstream cytokine capable of activating apoptotic pathways. Phosphorylation of AMPK has been reported to have inhibitory effects on ACC1 in humans and mice [33,34]. AKT is a central regulator of lipid metabolism and an upstream signaling molecule that adjusts the Akt/mTOR pathway to stimulate lipid accumulation [35]. Based on our experimental data, APOH regulates the expression of ACC1 by inactivating the AMPK pathway and activating the AKT pathway to regulate the synthesis of fatty acids.

There is evidence that activation of AMPK can inhibit the differentiation of adipocytes by blocking the transcription factor PPARG [36]. PPARG gene is involved in the process of adipocyte differentiation, which may be due to the activation of AKT[37]. PPARG is the primary regulator of adipogenesis. Our data show that overexpression of APOH reduces the expression of PPARG and ACSL1, and knockdown of APOH increases the expression of PPARG and ACSL1. APOH may reduce the β-oxidation of fatty acids through the PPARG pathway to cause the accumulation of TG in CS2s. These pathways are the leading promoters of TG and CHOL accumulation. A similar study showed that high expression of ACSL1 in human liver cells reduces the β-oxidation of fatty acids through the PPARG pathway, thereby increasing TG [38]. The overexpression of ACSL1 in cardiomyocytes will increase the content of TGs in cells, which suggests that ACSL1 gene is involved in the accumulation of TGs in cardiomyocytes[39]. These results are contrary to the results of this experiment, which may be due to the different cell types selected, and different cell samples have large differences in the process of TGs metabolism. The above research results show that APOH inhibits the expression of PPARG by regulating the AMPK/AKT pathway. As a transcription factor, PPARG can participate in controlling TG levels and free fatty acid formation by regulating the expression of ACSL1 [38,40].

LPL is the main enzyme that converts TG into free fatty acids and it has important functions [16]. It is well known that PPARG is a downstream signal molecule of AKT and a transcription factor involved in regulating lipid metabolism [41-43]. After the mouse very-low-density lipoprotein receptor (VLDL) receptor gene was knocked out, the expression of LPL was significantly reduced, leading to a significant increase in plasma TG content after meals, which indicated that LPL is involved in physiological process of TG clearance in mice [44]. When we regulate the expression of APOH gene in myoblasts, we found that APOH inhibits the expression of LPL through the AKT/PPARG pathway, reduces the clearance of TG in myoblasts, and causes the accumulation of TG in cells.

ELOVL6 is a particulate enzyme involved in the elongation of long-chain saturated and unsaturated fatty acids [45]. Studies have shown that ELOVL6 can catalyse lipid synthesis in bovine mammary epithelial cells [46]. ELOVL6 has a central role in obesity-induced insulin resistance by altering fatty acid composition and is a major target of hepatic sterol regulatory element-binding proteins [47]. In addition, the long-chain fatty acid metabolism driven by ELOVL6 is regulated by AMPK signal transduction [48]. This study showed that overexpression of APOH increased the expression of ELOVL6, while knockdown of APOH had the opposite result. This result indicates that APOH may stimulate the expression of ELOVL6 by inhibiting the activation of APMK, thereby promoting the synthesis of long-chain fatty acids in CS2s.

CONCLUSION

In summary, our results show that APOH inhibits the expression of PPARG and activating AKT, thereby inhibiting fatty acid oxidation, and at the same time, by inhibiting AMPK, it enhances the

https://doi.org/10.5187/jast.2022.e60

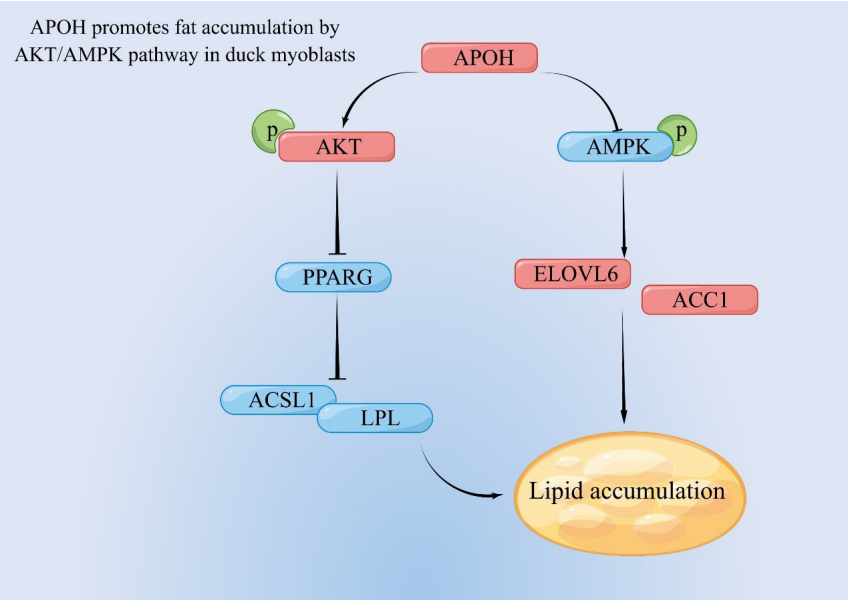

Fig. 9. APOH activating AKT and inhibits the expression of PPARG, ACSL1, and LPL, thereby inhibiting fatty acid oxidation, and at the same time, by inhibiting AMPK, it enhances the expression of ACC1 and ELOVL6 and promotes lipid accumulation. APOH, apolipoprotein H; AMPK, AMP-activated catalytic subunit alpha 1; PPARG, peroxisome proliferator activated receptor gamma; ELOVL6, ELOVL fatty acid elongase 6; ACC1, acetyl-CoA carboxylase 1; ACSL1, acyl-CoA synthetase long chain family member 1; LPL, lipoprotein lipase.

expression of ACC1 and ELOVL6 and promotes lipid synthesis (Fig. 9).

REFERENCES

1. Xing S, Liu R, Zhao G, Liu L, Groenen MAM, Madsen O, et al. RNA-seq analysis reveals hub genes involved in chicken intramuscular fat and abdominal fat deposition during development. Front Genet. 2020;11:1009. https://doi.org/10.3389/fgene.2020.01009
2. Ye Y, Lin S, Mu H, Tang X, Ou Y, Chen J, et al. Analysis of differentially expressed genes and signaling pathways related to intramuscular fat deposition in skeletal muscle of sex-linked dwarf chickens. BioMed Res Int. 2014;2014:724274. https://doi.org/10.1155/2014/724274
3. Qiu F, Xie L, Ma J, Luo W, Zhang L, Chao Z, et al. Lower expression of SLC27A1 enhances intramuscular fat deposition in chicken via down-regulated fatty acid oxidation mediated by CPT1A. Front Physiol. 2017;8:449. https://doi.org/10.3389/fphys.2017.00449
4. Guo Y, Guo X, Deng Y, Cheng L, Hu S, Liu H, et al. Effects of different rearing systems on intramuscular fat content, fatty acid composition, and lipid metabolism–related genes expression in breast and thigh muscles of Nonghua ducks. Poult Sci. 2020;99:4832-44. https://doi.org/10.1016/j.psj.2020.06.073
5. Stein O, Stein Y, Lefevre M, Roheim PS. The role of apolipoprotein A-IV in reverse cholesterol transport studied with cultured cells and liposomes derived from an ether analog of phosphatidylcholine. Biochim Biophys Acta Mol Cell Biol Lipids. 1986;878:7-13. https://doi.org/10.1016/0005-2760(86)90337-1
6. George J, Harats D, Gilburd B, Afek A, Levy Y, Schneiderman J, et al. Immunolocalization of β2-glycoprotein I (apolipoprotein H) to human atherosclerotic plaques: potential implications for lesion progression. Circulation. 1999;99:2227-30. https://doi.org/10.1161/01.

CIR.99.17.2227
7. Afek A, George J, Shoenfeld Y, Gilburd B, Levy Y, Shaish A, et al. Enhancement of atherosclerosis in beta-2-glycoprotein I-immunized apolipoprotein E-deficient mice. Pathobiology. 1999;67:19-25. https://doi.org/10.1159/000028046
8. Tsonkova VG, Sand FW, Wolf XA, Grunnet LG, Ringgaard AK, Ingvorsen C, et al. The EndoC-βH1 cell line is a valid model of human beta cells and applicable for screenings to identify novel drug target candidates. Mol Metab. 2018;8:144-57. https://doi.org/10.1016/j.molmet.2017.12.007
9. Hoekstra M, Chen HY, Rong J, Dufresne L, Yao J, Guo X, et al. Genome-wide association study highlights APOH as a novel locus for lipoprotein(a) levels—brief report. Arterioscler Thromb Vasc Biol. 2021;41:458-64. https://doi.org/10.1161/ATVBAHA.120.314965
10. Perrin RJ, Craig-Schapiro R, Malone JP, Shah AR, Gilmore P, Davis AE, et al. Identification and validation of novel cerebrospinal fluid biomarkers for staging early Alzheimer's disease. PLOS ONE. 2011;6:e16032. https://doi.org/10.1371/journal.pone.0016032
11. Song F, Poljak A, Crawford J, Kochan NA, Wen W, Cameron B, et al. Plasma apolipoprotein levels are associated with cognitive status and decline in a community cohort of older individuals. PLOS ONE. 2012;7:e34078. https://doi.org/10.1371/journal.pone.0034078
12. Nakaya Y, Schaefer EJ, Brewer HB Jr. Activation of human post heparin lipoprotein lipase by apolipoprotein H (β2-glycoprotein I). Biochem Biophys Res Commun. 1980;95:1168-72. https://doi.org/10.1016/0006-291x(80)91595-8
13. Schousboe I. Binding of β2-glycoprotein I to platelets: effect of adenylate cyclase activity. Thromb Res. 1980;19:225-37. https://doi.org/10.1016/0049-3848(80)90421-1
14. Nimpf J, Bevers EM, Bomans PHH, Till U, Wurm H, Kostner GM, et al. Prothrombinase activity of human platelets is inhibited by β2-glycoprotein-I. Biochim Biophys Acta Gen Subj. 1986;884:142-9. https://doi.org/10.1016/0304-4165(86)90237-0
15. Sha H, Sun S, Francisco AB, Ehrhardt N, Xue Z, Liu L, et al. The ER-associated degradation adaptor protein Sel1L regulates LPL secretion and lipid metabolism. Cell Metabol. 2014;20:458-70. https://doi.org/10.1016/j.cmet.2014.06.015
16. Yagyu H, Chen G, Yokoyama M, Hirata K, Augustus A, Kako Y, et al. Lipoprotein lipase (LpL) on the surface of cardiomyocytes increases lipid uptake and produces a cardiomyopathy. J Clin Invest. 2003;111:419-26. https://doi.org/doi.org/10.1172/JCI16751
17. Yuan SM, Guo Y, Wang Q, Xu Y, Wang M, Chen HN, et al. Over-expression of PPAR-γ2 gene enhances the adipogenic differentiation of hemangioma-derived mesenchymal stem cells in vitro and in vivo. Oncotarget. 2017;8:115817-28. https://doi.org/10.18632/oncotarget.23705
18. Zhong J, Gong W, Lu L, Chen J, Lu Z, Li H, et al. Irbesartan ameliorates hyperlipidemia and liver steatosis in type 2 diabetic db/db mice via stimulating PPAR-γ, AMPK/Akt/mTOR signaling and autophagy. Int Immunopharmacol. 2017;42:176-84. https://doi.org/10.1016/j.intimp.2016.11.015
19. He C, Zhang G, Ouyang H, Zhang P, Chen Y, Wang R, et al. Effects of β2/aβ2 on oxLDL-induced CD36 activation in THP-1 macrophages. Life Sci. 2019;239:117000. https://doi.org/10.1016/j.lfs.2019.117000
20. Chawla A, Barak Y, Nagy L, Liao D, Tontonoz P, Evans RM. PPAR-γ dependent and independent effects on macrophage-gene expression in lipid metabolism and inflammation. Nat Med. 2001;7:48-52. https://doi.org/10.1038/83336
21. Guo L, Cui H, Zhao G, Liu R, Li Q, Zheng M, et al. Intramuscular preadipocytes impede differentiation and promote lipid deposition of muscle satellite cells in chickens. BMC Genomics. 2018;19:838. https://doi.org/10.1186/s12864-018-5209-5

https://doi.org/10.5187/jast.2022.e60

22. Jin S, Xu Y, Zang H, Yang L, Lin Z, Li Y, et al. Expression of genes related to lipid transport in meat-type ducks divergent for low or high residual feed intake. Asian-Australas J Anim Sci. 2020;33:416-23. https://doi.org/10.5713/ajas.19.0284
23. Xu S, Huang Y, Xie Y, Lan T, Le K, Chen J, et al. Evaluation of foam cell formation in cultured macrophages: an improved method with Oil Red O staining and DiI-oxLDL uptake. Cytotechnology. 2010;62:473-81. https://doi.org/10.1007/s10616-010-9290-0
24. Shaw CS, Clark J, Wagenmakers AJM. The effect of exercise and nutrition on intramuscular fat metabolism and insulin sensitivity. Annu Rev Nutr. 2010;30:13-34. https://doi.org/10.1146/annurev.nutr.012809.104817
25. Mihaylova MM, Shaw RJ. The AMPK signalling pathway coordinates cell growth, autophagy and metabolism. Nat Cell Biol. 2011;13:1016-23. https://doi.org/10.1038/ncb2329
26. Machann J, Häring H, Schick F, Stumvoll M. Intramyocellular lipids and insulin resistance. Diabetes Obes Metab. 2004;6:239-48. https://doi.org/10.1111/j.1462-8902.2004.00339.x
27. Moro C, Bajpeyi S, Smith SR. Determinants of intramyocellular triglyceride turnover: implications for insulin sensitivity. Am J Physiol Endocrinol Metab. 2008;294:E203-13. https://doi.org/10.1152/ajpendo.00624.2007
28. Jacobsen SC, Brøns C, Bork-Jensen J, Ribel-Madsen R, Yang B, Lara E, et al. Effects of short-term high-fat overfeeding on genome-wide DNA methylation in the skeletal muscle of healthy young men. Diabetologia. 2012;55:3341-9. https://doi.org/10.1007/s00125-012-2717-8
29. Liu J, Fu R, Liu R, Zhao G, Zheng M, Cui H, et al. Protein profiles for muscle development and intramuscular fat accumulation at different post-hatching ages in chickens. PLOS ONE. 2016;11:e0159722. https://doi.org/10.1371/journal.pone.0159722
30. Reyer H, Metzler-Zebeli BU, Trakooljul N, Oster M, Muráni E, Ponsuksili S, et al. Transcriptional shifts account for divergent resource allocation in feed efficient broiler chickens. Sci Rep. 2018;8:12903. https://doi.org/10.1038/s41598-018-31072-7
31. Castro A, Lázaro I, Selva DM, Céspedes E, Girona J, Plana N, et al. APOH is increased in the plasma and liver of type 2 diabetic patients with metabolic syndrome. Atherosclerosis. 2010;209:201-5. https://doi.org/10.1016/j.atherosclerosis.2009.09.072
32. Wang X, Li Y, Chen X, Zhou Z, Yao J. Human acetyl-CoA carboxylase 1 is an isomerase: carboxyl transfer is activated by catalytic effect of isomerization. J Phys Chem B. 2019;123:6757-64. https://doi.org/10.1021/acs.jpcb.9b05384
33. Fullerton MD, Galic S, Marcinko K, Sikkema S, Pulinilkunnil T, Chen ZP, et al. Single phosphorylation sites in Acc1 and Acc2 regulate lipid homeostasis and the insulin-sensitizing effects of metformin. Nat Med. 2013;19:1649-54. https://doi.org/10.1038/nm.3372
34. Tyszka-Czochara M, Konieczny P, Majka M. Recent advances in the role of AMP-activated protein kinase in metabolic reprogramming of metastatic cancer cells: targeting cellular bioenergetics and biosynthetic pathways for anti-tumor treatment. J Physiol Pharmacol. 2018;69:337-49. https://doi.org/10.26402/jpp.2018.3.07
35. Du C, Wu M, Liu H, Ren Y, Du Y, Wu H, et al. Thioredoxin-interacting protein regulates lipid metabolism via Akt/mTOR pathway in diabetic kidney disease. Int J Biochem Cell Biol. 2016;79:1-13. https://doi.org/10.1016/j.biocel.2016.08.006
36. Habinowski SA, Witters LA. The effects of AICAR on adipocyte differentiation of 3T3-L1 cells. Biochem Biophys Res Commun. 2001;286:852-6. https://doi.org/10.1006/bbrc.2001.5484
37. Jiang T, Shi X, Yan Z, Wang X, Gun S. Isoimperatorin enhances 3T3-L1 preadipocyte differentiation by regulating PPARγ and C/EBPα through the Akt signaling pathway. Exp Ther Med. 2019;18:2160-6. https://doi.org/10.3892/etm.2019.7820

38. Li T, Li X, Meng H, Chen L, Meng F. ACSL1 affects triglyceride levels through the PPARγ pathway. Int J Med Sci. 2020;17:720-7. https://doi.org/10.7150/ijms.42248
39. Singh AB, Kan CFK, Dong B, Liu J. SREBP2 activation induces hepatic long-chain acyl-CoA synthetase 1 (ACSL1) expression in vivo and in vitro through a sterol regulatory element (SRE) motif of the ACSL1 C-promoter. J Biol Chem. 2016;291:5373-84. https://doi.org/10.1074/jbc.m115.696872
40. Yan G, Li X, Peng Y, Long B, Fan Q, Wang Z, et al. The fatty acid β-oxidation pathway is activated by leucine deprivation in HepG2 cells: a comparative proteomics study. Sci Rep. 2017;7:1914. https://doi.org/10.1038/s41598-017-02131-2
41. Manning BD, Toker A. AKT/PKB signaling: navigating the network. Cell. 2017;169:381-405. https://doi.org/10.1016/j.cell.2017.04.001
42. Peng X, Chen R, Wu Y, Huang B, Tang C, Chen J, et al. PPARγ–PI3K/AKT–NO signal pathway is involved in cardiomyocyte hypertrophy induced by high glucose and insulin. J Diabetes Complications. 2015;29:755-60. https://doi.org/10.1016/j.jdiacomp.2015.04.012
43. Bermudez B, Dahl TB, Medina I, Groeneweg M, Holm S, Montserrat-de la Paz S, et al. Leukocyte overexpression of intracellular NAMPT attenuates atherosclerosis by regulating PPARγ-dependent monocyte differentiation and function. Arterioscler Thromb Vasc Biol. 2017;37:1157-67. https://doi.org/10.1161/ATVBAHA.116.308187
44. Goudriaan JR, Espirito Santo SM, Voshol PJ, Teusink B, van Dijk KW, van Vlijmen BJM, et al. The VLDL receptor plays a major role in chylomicron metabolism by enhancing LPL-mediated triglyceride hydrolysis. J Lipid Res. 2004;45:1475-81. https://doi.org/10.1194/jlr.M400009-JLR200
45. Matsuzaka T, Shimano H. Elovl6: a new player in fatty acid metabolism and insulin sensitivity. J Mol Med. 2009;87:379-84. https://doi.org/10.1007/s00109-009-0449-0
46. Fan X, Zhu W, Qiu L, Zhang G, Zhang Y, Miao Y. Elongase of very long chain fatty acids 6 (ELOVL6) promotes lipid synthesis in buffalo mammary epithelial cells. J Anim Physiol Anim Nutr. 2022;106:1-11. https://doi.org/10.1111/jpn.13536
47. Matsuzaka T, Atsumi A, Matsumori R, Nie T, Shinozaki H, Suzuki-Kemuriyama N, et al. Elovl6 promotes nonalcoholic steatohepatitis. Hepatology. 2012;56:2199-208. https://doi.org/10.1002/hep.25932
48. Sunaga H, Matsui H, Anjo S, Syamsunarno MRAA, Koitabashi N, Iso T, et al. Elongation of long-chain fatty acid family member 6 (Elovl6)-driven fatty acid metabolism regulates vascular smooth muscle cell phenotype Tthrough AMP-activated protein kinase/Krüppel-like factor 4 (AMPK/KLF4) signaling. J Am Heart Assoc. 2016;5:e004014. https://doi.org/10.1161/JAHA.116.004014

https://doi.org/10.5187/jast.2022.e60